Electronic Supplementary Material (ESI) for Physical Chemistry Chemical Physics.

Supporting Information

Appraising the Potency of Small Molecule Inhibitors and Their Graphene Surface-Mediated Organizational Attributes on Uric Acid-Melamine Clusters

Krishna Gopal Chattaraj and Sandip Paul*

Department of Chemistry, Indian Institute of Technology, Guwahati Assam, India-781039

Number of pages: 27

Number of figures: 23

Number of schemes: 0

Number of tables: 5

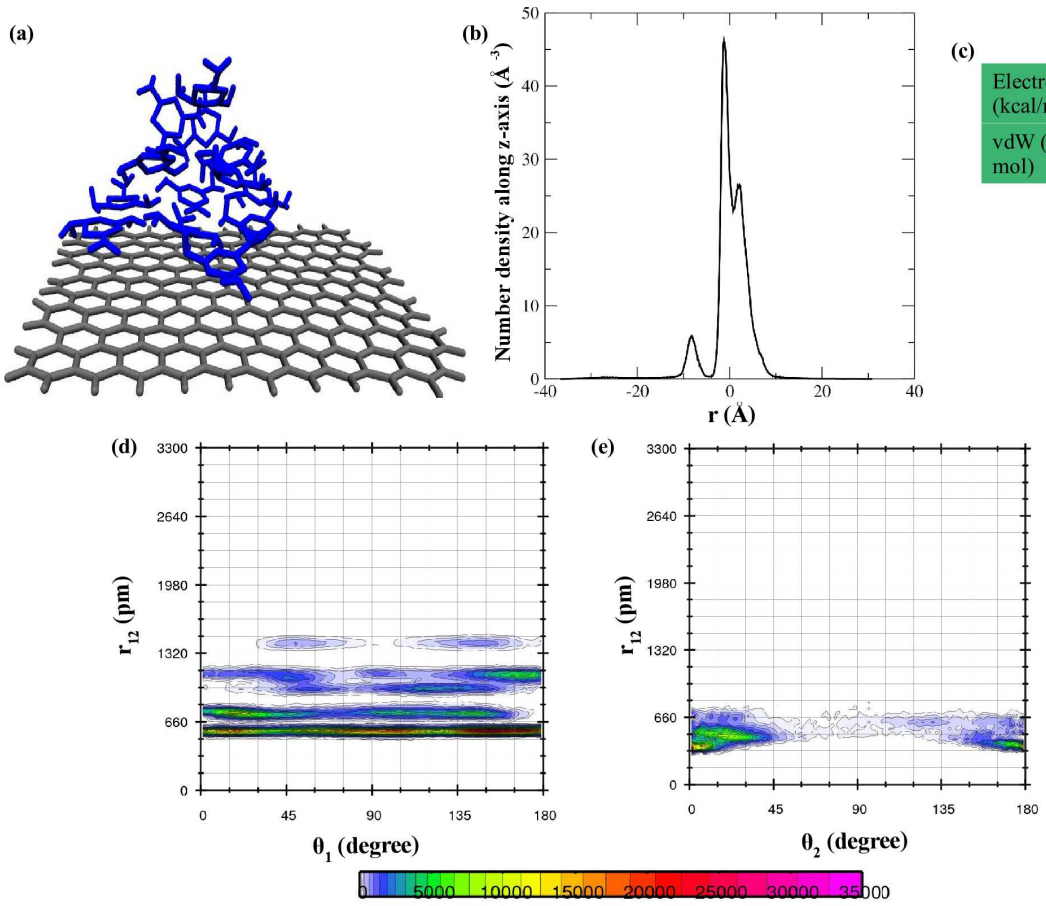

FIG. S1: (a) In system M15G1, 13 out of 15 MM molecules are adsorbed on the graphene surface. Again, 7 MM molecules are adsorbed in the first layer of graphene. The remaining molecules are adsorbed over the first layer. Here, two molecules can form a dimer over the graphene surface during the cluster structure analysis only when they are attached by either hydrogen bonding or π- stacking interactions. The first layer of graphene surface is considered as a surface that at 4 Å of distance from that monolayer graphene surface, (b) the number density of MM molecules over the graphene along the z-direction in system M15G1, (c) the decomposition of total energy into its two components (i.e., electrostatic and vdW energies). The energy is expressed in kcal/mol unit, (d) the distribution of orientational angle (θ_1) between two MM molecules considering two-point vectors (i.e., the vector connected by a donor (D), hydrogen (H), and acceptor (A) atoms of these two molecules) to describe the hydrogen bonding phenomenon, and (e) the angle between two vector normals (θ_2) between two aromatic rings is shown to present the π-stacking. Here, r_{12} refers to the center of mass (COM)- center of mass (COM) distance between the individual molecules.

(a)

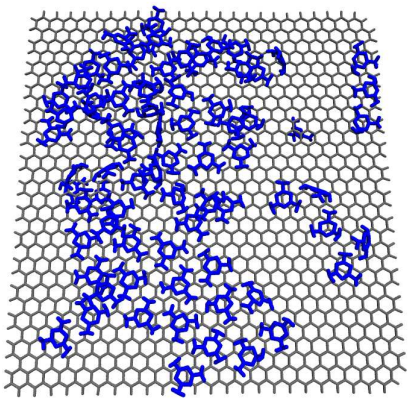

(b)

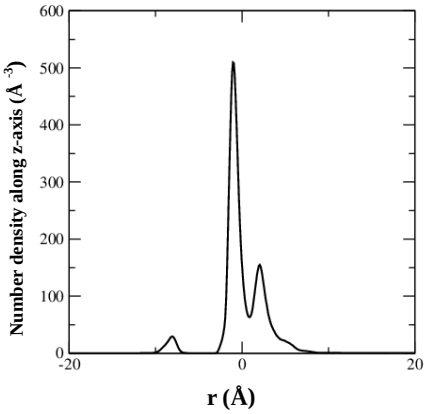

(c)

Electrostatic (kcal/mol)	0.0
vdW (kcal/mol)	-240.88

FIG. S2: (a) In system M75G2, 53 MM molecules are adsorbed in the first layer of graphene, whereas 72 out of 75 MM molecules are adsorbed in all layers in total. Here, during the cluster structure analysis, two molecules can form a dimer over the graphene surface only when they are attached by either hydrogen bonding or π- stacking interactions. The first layer of graphene surface is considered a surface at 4 Å of distance from that monolayer graphene surface, (b) the number density of MM molecules over the graphene along the z-direction in system M75G2, and (c) the decomposition of total energy into its two components (i.e., electrostatic and vdW energies). The energy is expressed in kcal/mol unit.

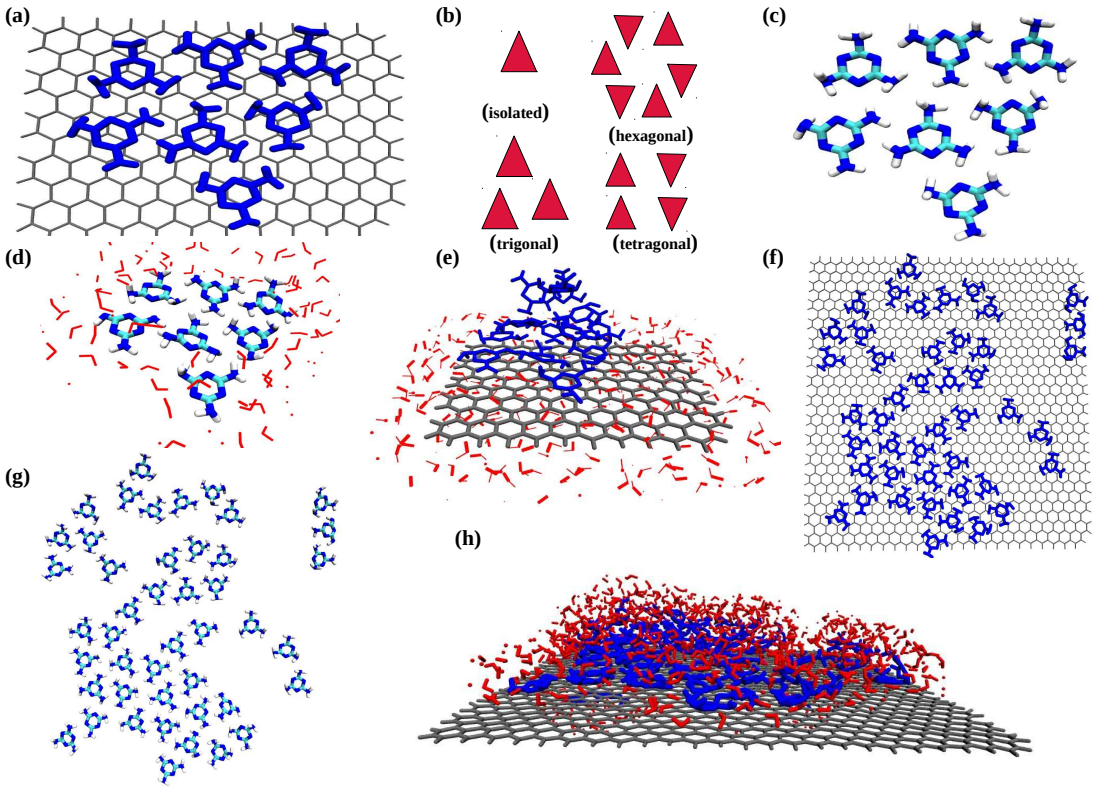

FIG. S3: (a) The first layer of adsorption by MM molecules over a monolayer graphene surface in system M15G1, (b) during the adsorption of MM molecules over a single layer graphene surface, they can form various patterns (i.e., single-molecule adsorption, trigonal, hexagonal, and tetragonal patterns with the increase of surface area coverage) to form large 2D supermolecular shape, (c) hydrogen-bonded MM molecules over the graphene surface in system M15G1, (d)-(e) surface adsorbed water molecules surround MM molecules within 3.5 Å from MM and 5 Å from the graphene surface in system M15G1, (f)-(g) in system M75G2, in the first layer of adsorption by MM molecules and it can be seen that the surface coverage is not extensive as MM molecules are associated with water molecules, and (h) surrounding water molecules over and around the graphene and MM molecules in system M75G2.

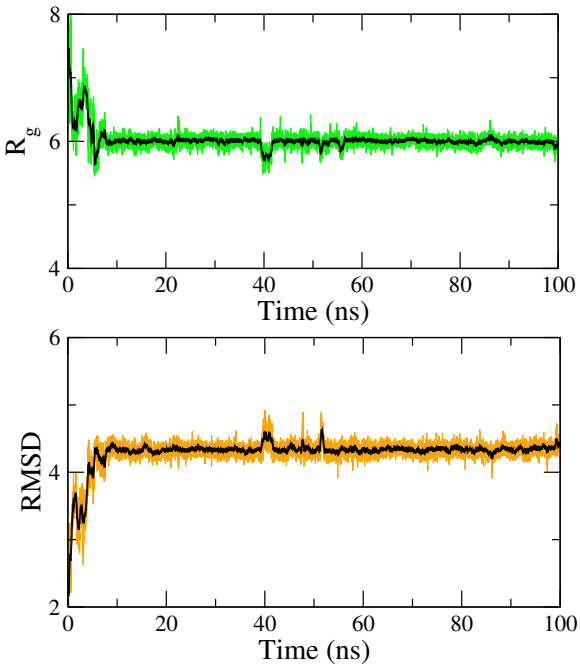

FIG. S4: The radius of gyration (R_g (Å), upper panel) and root means square deviation (RMSD (Å), lower panel) of MM molecules adsorbed in the first layer for system M75G2.

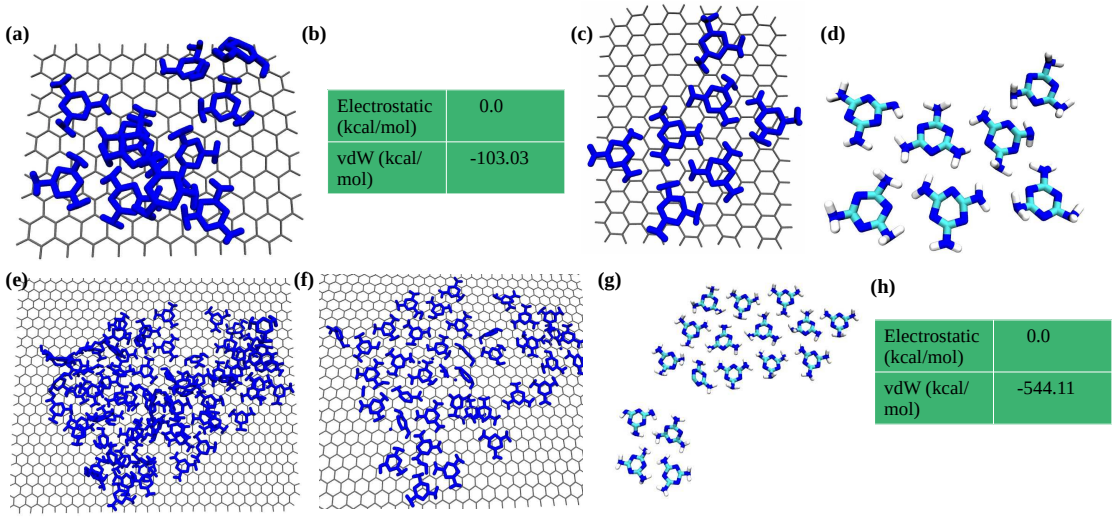

FIG. S5: (a) 7 MM molecules are adsorbed at the first layer of graphene. In comparison, a total of 11 MM molecules are attached with the graphene surface in all layers in system M15G1-a, (b) MM molecules produce a strong vdW interaction with the graphene surface, (c)-(d) In the unit cell pattern, here in system M15G1-a, a similar way with no definite large assembly over the graphene surface is formed as like system M15G1, (e) Like the M75G2 system, in system M75G2-a, an equivalent number of adsorbed MM molecules over the graphene surface can be found, (f)-(g) the composition of the adsorbed MM molecules in the first layer and their adsorption pattern in system M75G2-a, and (h) the decomposition of total energy into its two components in system M75G2-a (i.e., electrostatic and vdW energies). The energy is expressed in kcal/mol unit.

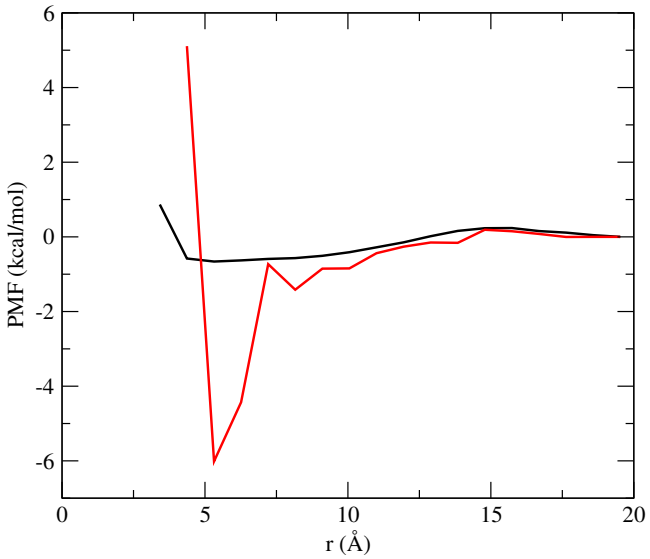

FIG. S6: The potentials of mean forces for systems M1G1-a (black) and M10G1-a (red).

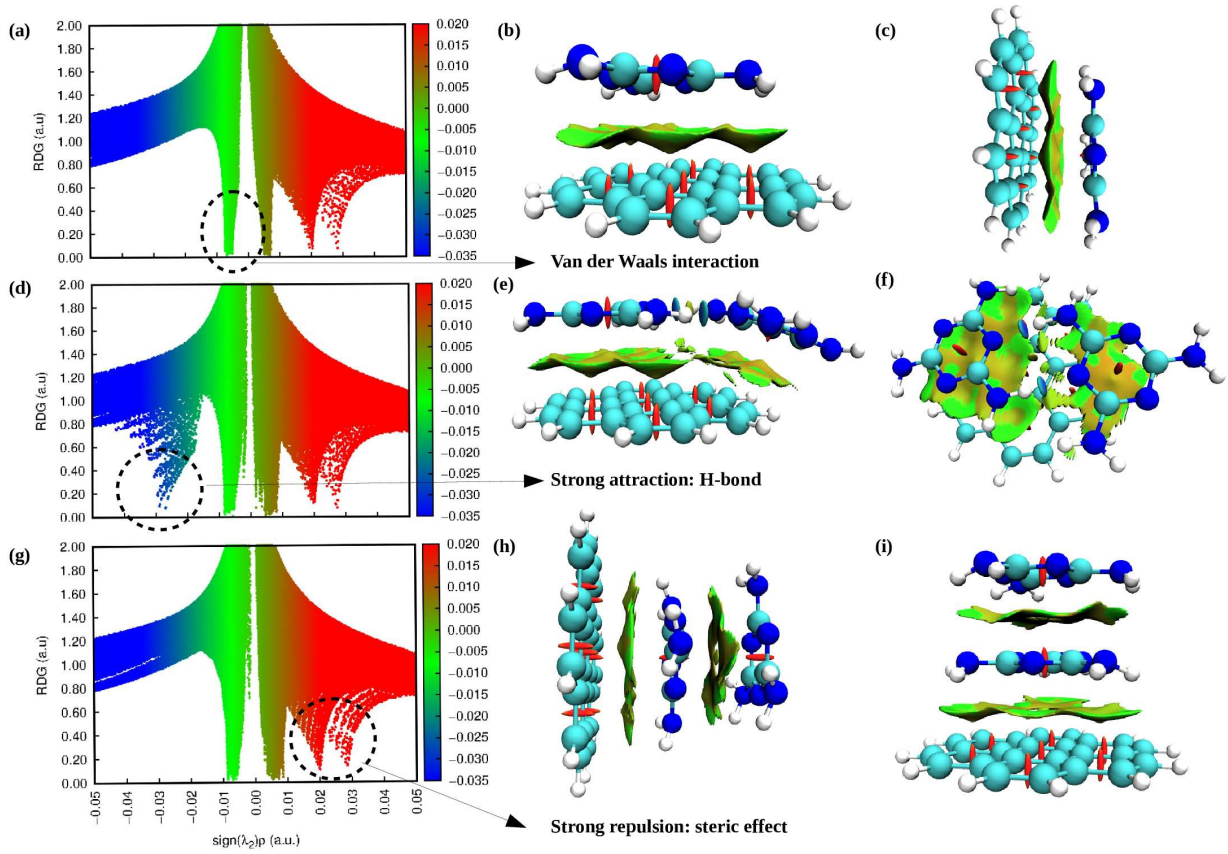

FIG. S7: Color-filled RDG isosurface reciprocates noncovalent interaction (NCI) regions for various interactions between MM and coronene system. (a)-(c) A single MM molecule is adsorbed over a coronene surface, (d)-(f) two hydrogen-bonded MM molecules are adsorbed over a coronene surface, and (g)-(i) two π-stacked MM molecules are adsorbed over a coronene surface. The vertical axis of this plot is the reduced density gradient (RDG), and the horizontal axis is the sign of the second largest eigenvalue of the electron density Hessian matrix at position r (sign($\lambda_2(\rho)$). Here, the strong repulsive non-bonded steric interaction is observed in the red, and attractive interactions like the hydrogen bonding and van der Waals are blue and green.

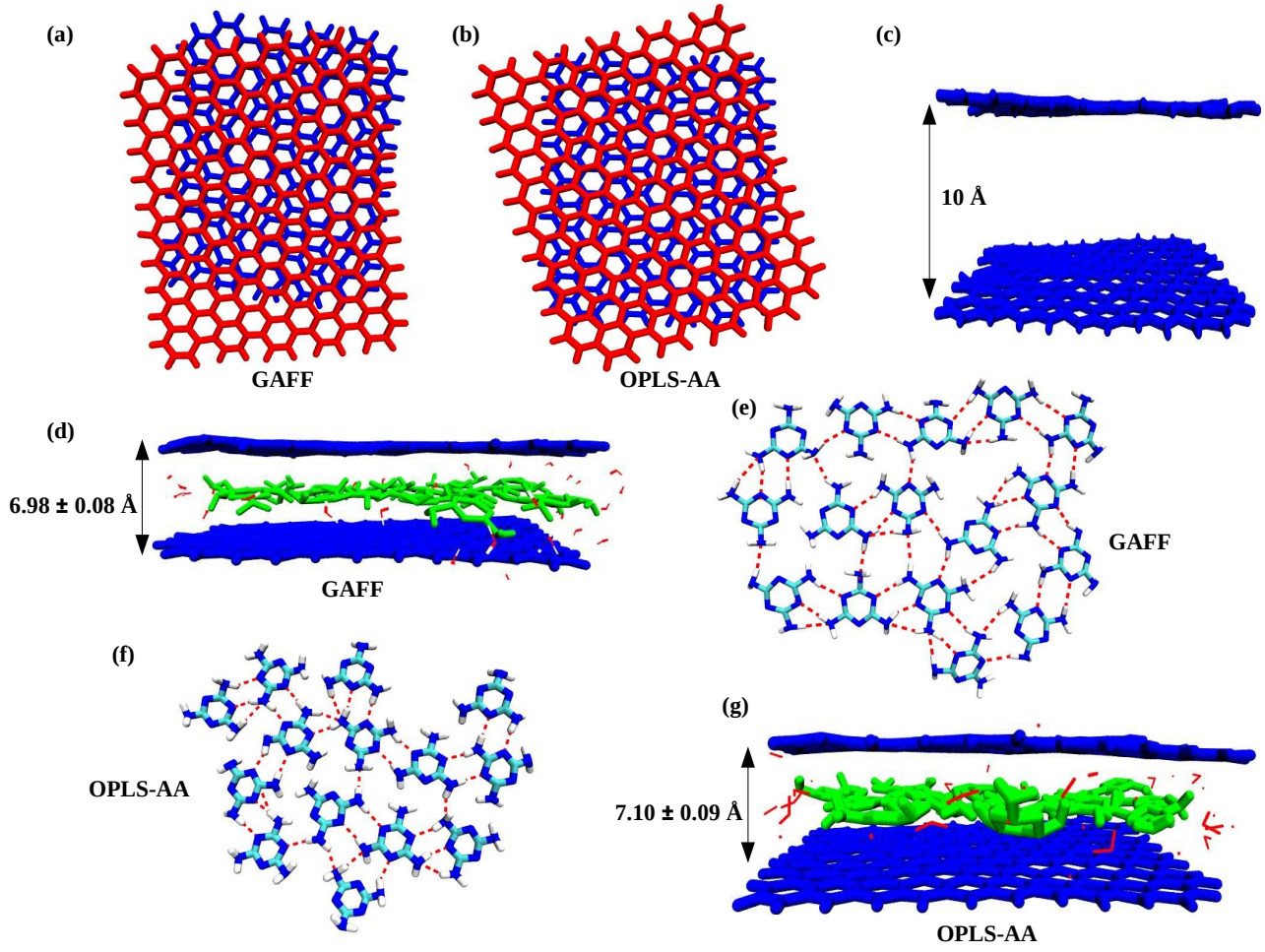

FIG. S8: The lateral displacement of the graphene sheet (in the xy direction) present in system (a) M40G12 and (b) M40G12-a, (c) intial graphene sheet seperation, (d) displacement of the movable graphene sheet in the presence of MM molecules in system M40G12, (e) pattern of adsorption of MM molecules in between two graphene sheets in system M40G12, (f) pattern of adsorption of MM molecules in between two graphene sheets in system M40G12-a, (g)displacement of the movable graphene sheet in the presence of MM molecules in system M40G12-a.

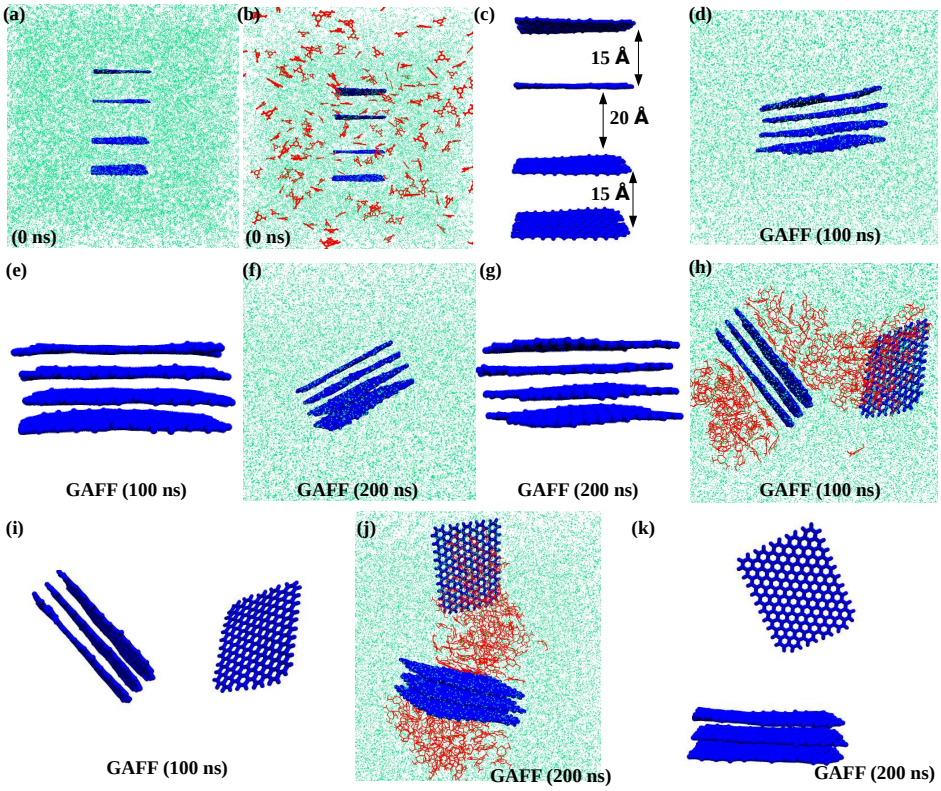

FIG. S9: (a) Initial configuration of graphene sheets surrounded by water (green) in system M0G14, (b) initial configuration of graphene sheets surrounded by water (green) in the presence of MM in system M200G14, (c) the initial separations among graphene sheets in systems M0G14 and M200G14, (d) the aggregated graphene nanosheets in solution at 100 ns simulation run in system M0G14, (e) the aggregated graphene nanosheets at 100 ns simulation run in system M0G14 (water molecules are left out for better visual clarity), (f) the aggregated graphene nanosheets in solution at 200 ns simulation run in system M0G14, (g) the aggregated graphene nanosheets at 200 ns simulation run in system M0G14 (water molecules are left out for better visual clarity), (h) the aggregated graphene nanosheets surrounded by water (green) in the presence of MM at 100 ns simulation run in system M200G14, (i) the aggregated graphene nanosheets at 100 ns simulation run in system M200G14 (water and MM molecules are left out for better visual clarity), (j) the aggregated graphene nanosheets surrounded by water (green) in the presence of MM at 200 ns simulation run in system M200G14, (k) the aggregated graphene nanosheets at 200 ns simulation run in system M200G14 (water and MM molecules are left out for better visual clarity).

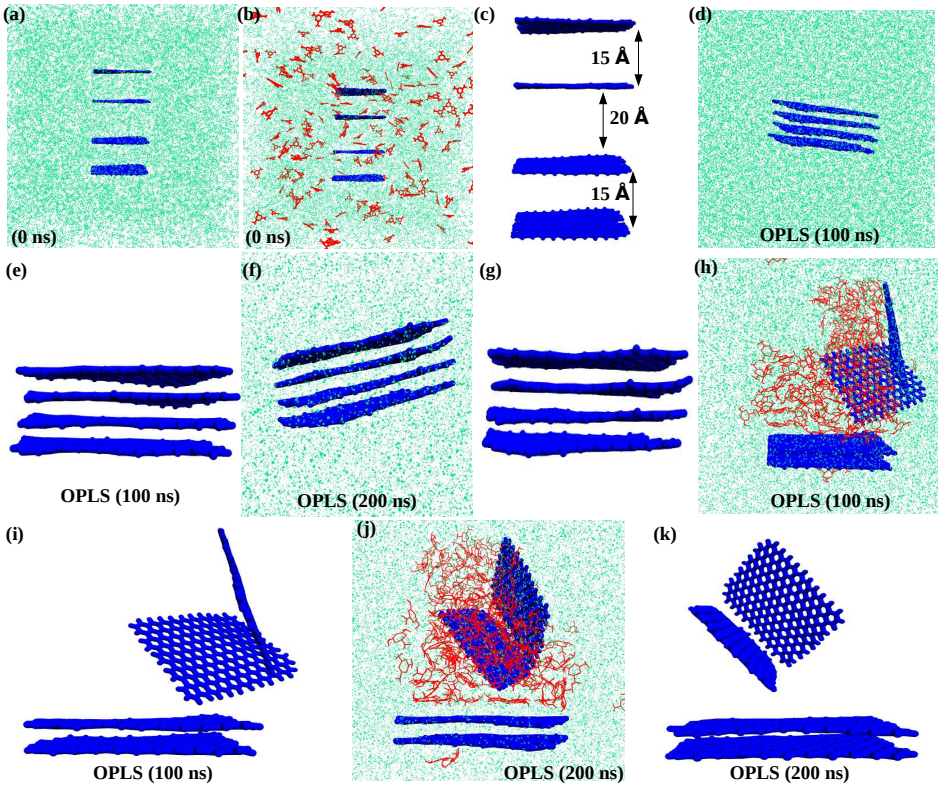

FIG. S10: (a) Initial configuration of graphene sheets surrounded by water (green) in system M0G14-a, (b) initial configuration of graphene sheets surrounded by water (green) in the presence of MM in system M200G14-a, (c) the initial separations among graphene sheets in systems M0G14-a and M200G14-a, (d) the aggregated graphene nanosheets in solution at 100 ns simulation run in system M0G14-a, (e) the aggregated graphene nanosheets at 100 ns simulation run in system M0G14-a (water molecules are left out for better visual clarity), (f) the aggregated graphene nanosheets in solution at 200 ns simulation run in system M0G14-a, (g) the aggregated graphene nanosheets at 200 ns simulation run in system M0G14-a (water molecules are left out for better visual clarity), (h) the aggregated graphene nanosheets surrounded by water (green) in the presence of MM at 100 ns simulation run in system M200G14-a, (i) the aggregated graphene nanosheets at 100 ns simulation run in system M200G14-a (water and MM molecules are left out for better visual clarity), (j) the aggregated graphene nanosheets surrounded by water (green) in the presence of MM at 200 ns simulation run in system M200G14-a, (k) the aggregated graphene nanosheets at 200 ns simulation run in system M200G14-a (water and MM molecules are left out for better visual clarity). Here, in the case of OPLS-AA parameters, both systems' (i.e., systems M0G14-a and M200G14-a) initial configurations are the same as that of the systems made of GAFF parameters (i.e., systems M0G14 and M200G14).

system	unconstrained exfoliating graphene
M40G12	0.03
M40G12-a	0.04

TABLE S1: Exfoliation diffusion coefficients ($\times 10^{-9}$ m^2/s) of graphene sheet in the presence of MM for systems M40G12 and M40G12-a.

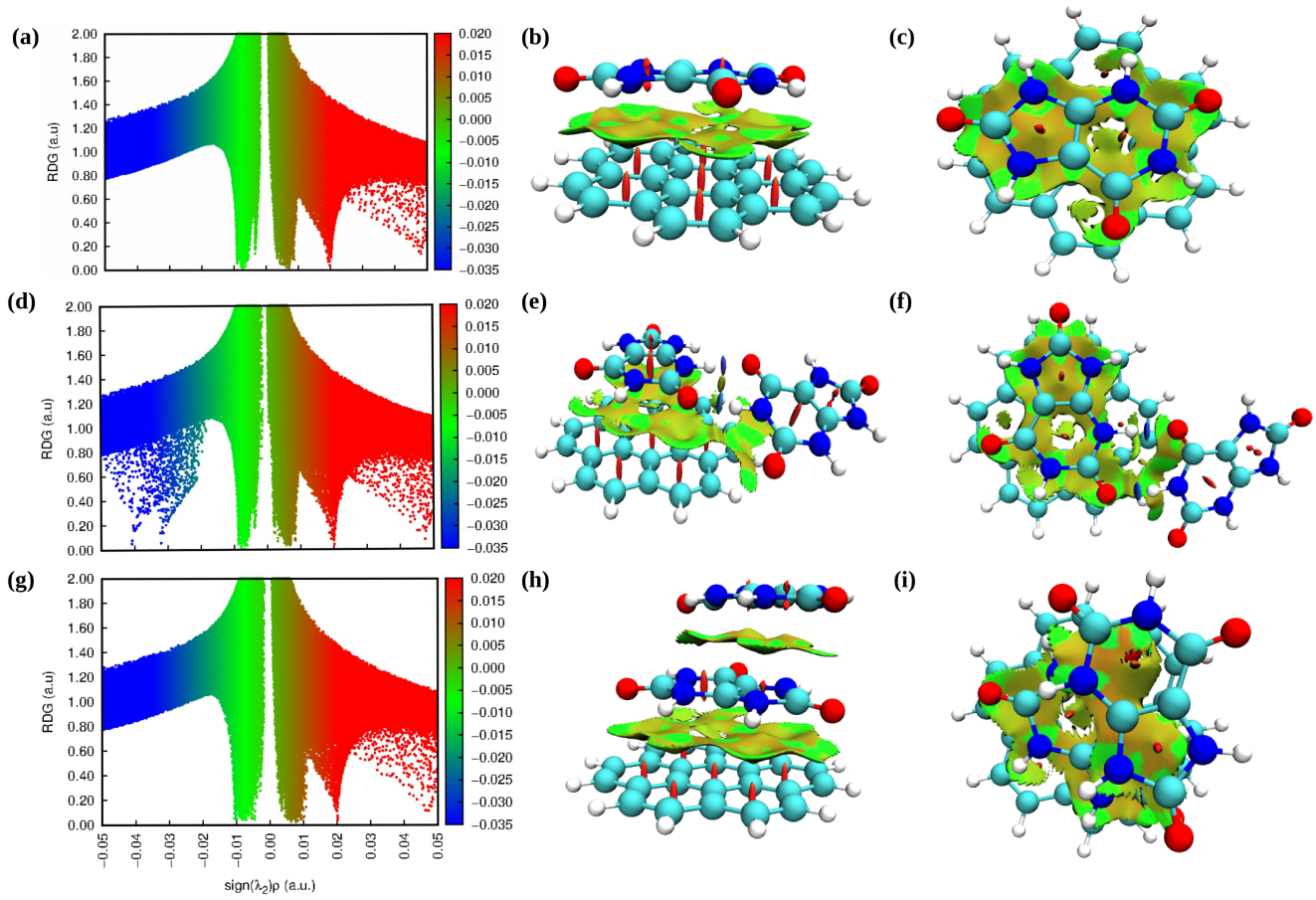

FIG. S11: Color-filled RDG isosurface reciprocates noncovalent interaction (NCI) regions for various interactions between UA and coronene system. (a)-(c) A single UA molecule is adsorbed over a coronene surface, (d)-(f) two hydrogen bonded UA molecules are adsorbed over a coronene surface, and (g)-(i) two π-stacked UA molecules are adsorbed over a coronene surface. The vertical axis of this plot is the reduced density gradient (RDG), and the horizontal axis is the sign of the second largest eigenvalue of the electron density Hessian matrix at position r (sign($\lambda_2(\rho)$)). Here, the strong repulsive non-bonded steric interaction is observed in the red, and attractive interactions like the hydrogen bonding and van der Waals are blue and green.

system	UA-UA	UA-MM	UA-TB	TB-MM	TB-TB	MM-MM
T0	43.48	75.93	—	—	—	43.21
T40	29.11	47.07	24.55	28.21	10.22	34.23

TABLE S2: The total number of hydrogen bonds between various pairs in the respective systems.

T0		T15			T40		
Energy	UA-MM	UA-MM	UA-TB	TB-MM	UA-MM	UA-TB	TB-MM
electrostatic	-438.84	-367.94	-204.67	-92.02	-288.75	-222.67	-161.03
vdW	-109.16	-54.84	-47.68	-24.87	-54.32	-188.24	-71.95

TABLE S3: The decompostion of total energy into its two components (i.e., electrostatic and vdW energies) for numerous pais. The energy is expreseed in kcal/mol unit.

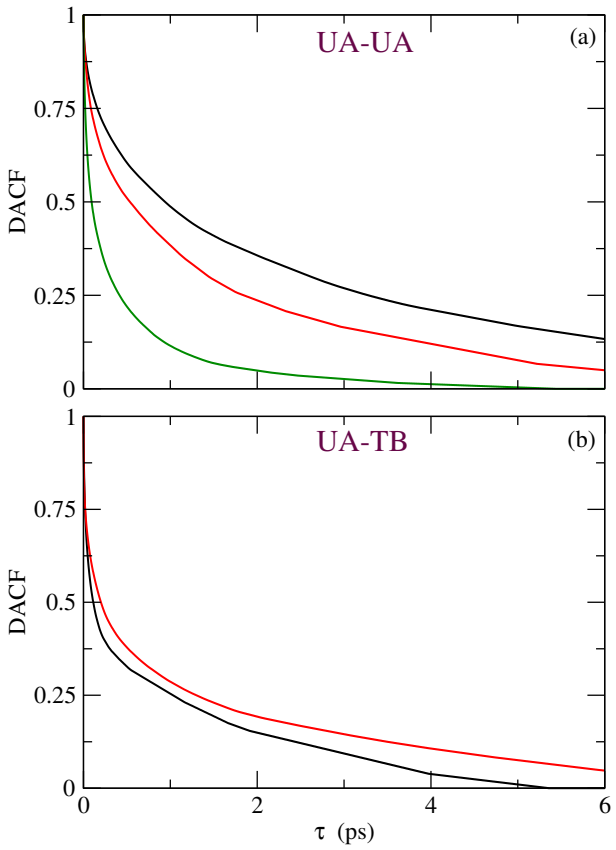

FIG. S12: DACF for (a) UA-UA (upper pannel) pair for systems T0 (black), T15 (red), and T40 (green) and (b) DACF for UA-TB (lower pannel) pair for systems T15 (black) and T40 (red).

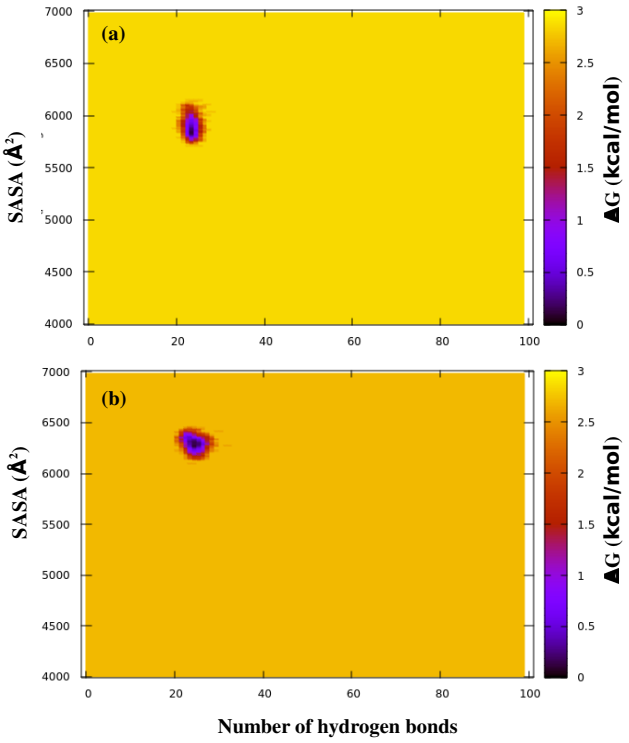

FIG. S13: Free energy landscape for the solvent-accessible surface area (SASA ($\mathring{A}^2$)) for UA-UA aggregation versus UA-TB hydrogen bonding for systems (a) T15 and (b) T40. The free energy in the color bar on the right side is manifested in kcal/mol unit.

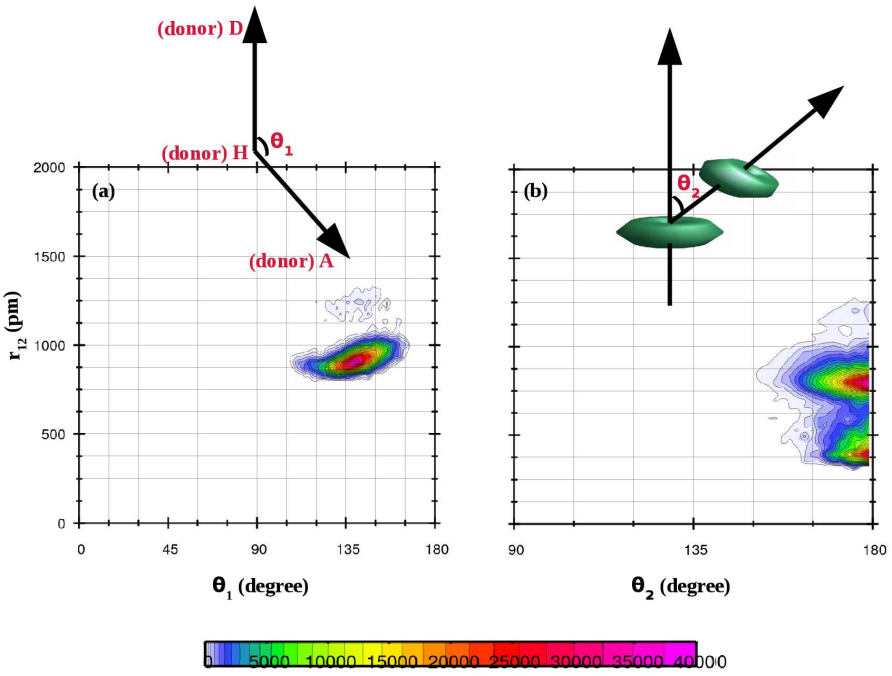

FIG. S14: In system T40, the distribution of orientational angle (θ_1) between UA and TB molecules considering two-point vectors (i.e. the vector connected by donor (D), hydrogen (H), and acceptor (A) atomes of these two molecules) to describe the hydrogen bonding phenomenon, and (e) The angle between two vector normals (θ_2) between two aromatic ring is shown to present the π-stacking. Here, r_{12} refers to the center of mass (COM)-center of mass (COM) distance between the respective molecules.

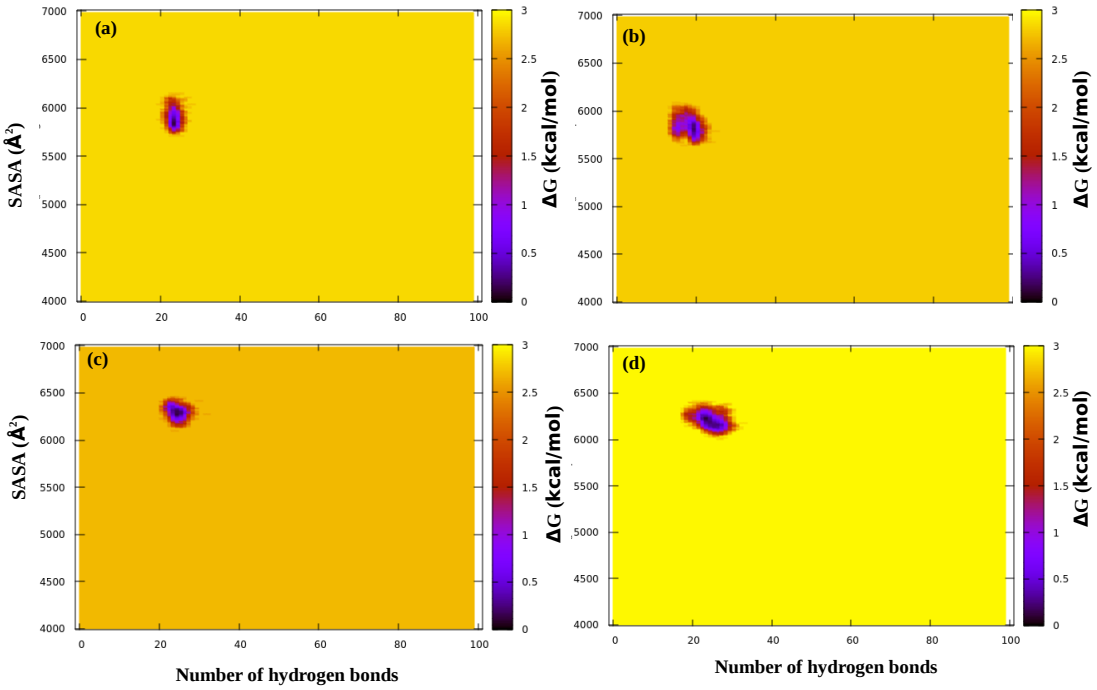

FIG. S15: Free energy landscape for the solvent-accessible surface area (SASA ($\mathring{A}^2$)) for UA-UA aggregation versus UA-TB hydrogen bonding for systems (a) T15, (b) T15-a, (c) T40, and (d) T40-a. The free energy in the color bar on the right side is manifested in kcal/mol unit.

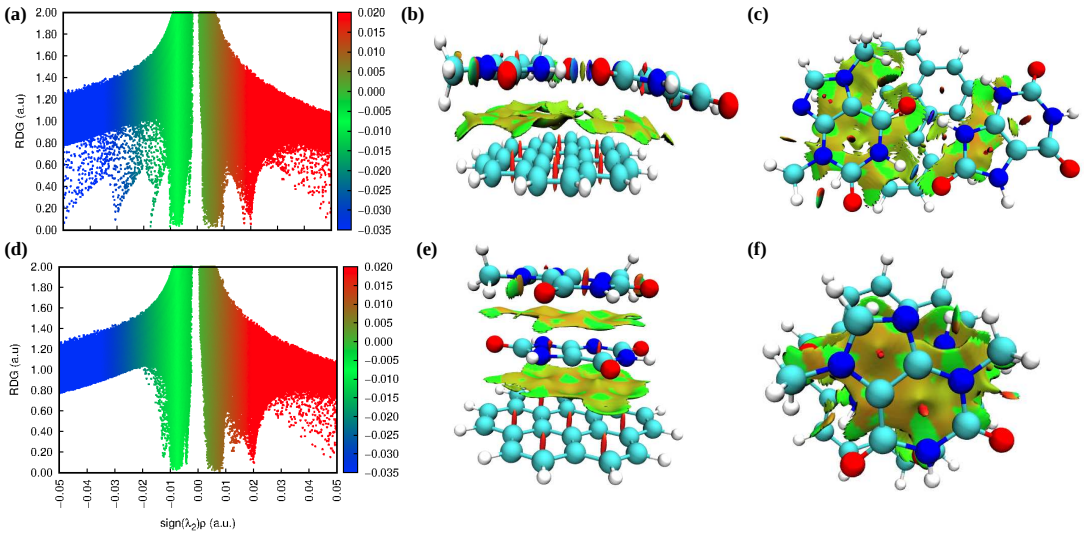

FIG. S16: Color-filled RDG isosurface reciprocates noncovalent interaction (NCI) regions for various interactions among UA, TB, and coronene system. (a)-(c) two hydrogen bonded UA and TB molecules are adsorbed over a coronene surface, and (d)-(f) two π-stacked UA and TB molecules are adsorbed over a coronene surface. The vertical axis of this plot is the reduced density gradient (RDG), and the horizontal axis is the sign of the second largest eigenvalue of the electron density Hessian matrix at position r (sign($\lambda_2(\rho)$). Here, the strong repulsive non-bonded steric interaction is observed in the red, and attractive interactions like the hydrogen bonding and van der Waals are blue and green.

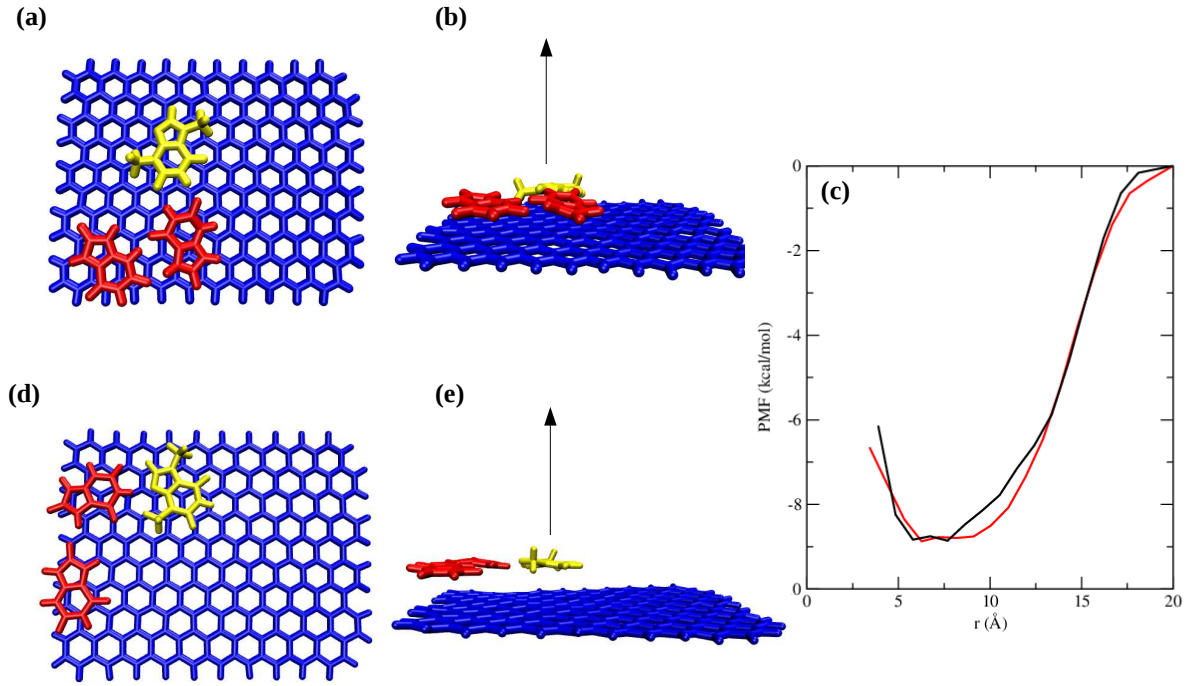

FIG. S17: (a) UA (red) and TB (yellow) molecules are adsorbed on a graphene surface in system U2T1G1, (b) TB molecule is pulled up from UA molecules in system U2T1G1, (c) PMFs for UA and TB interaction in systems U2T1G1 (black) and U2T1G1-a (red), (d) UA (red) and TB (yellow) molecules are adsorbed on a graphene surface in system U2T1G1-a, and (e) TB molecule is pulled up from UA molecules in system U2T1G1-a.

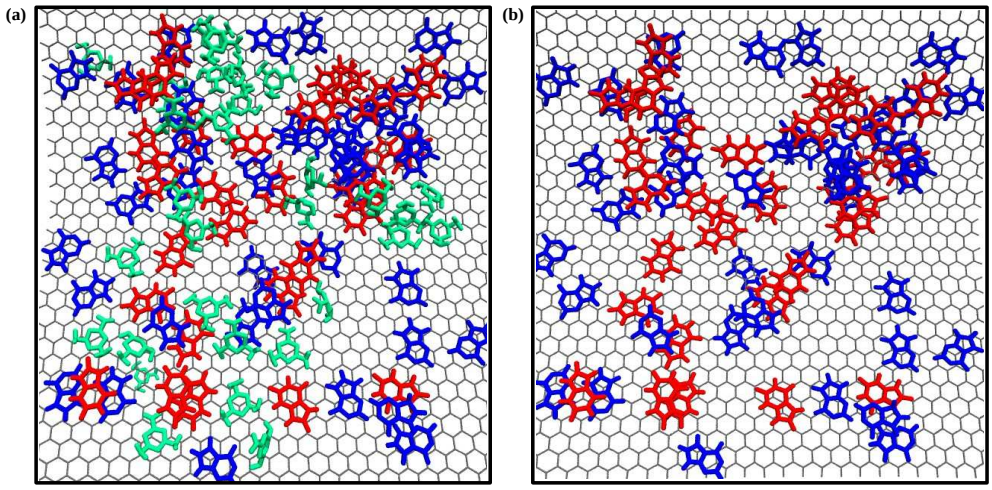

FIG. S18: (a) AP (blue) molecules disseminate themselves between UA (red) and MM (green) molecules and bind them to repress UA-MM aggregation, (b) orientaion of AP and UA molecules in system A40.

system	UA-UA	UA-MM	UA-AP	AP-MM	AP-AP	MM-MM
T0	43.48	75.93	—	—	—	43.21
A40	17.13	55.68	47.10	33.19	19.43	39.79

TABLE S4: The total number of hydrogen bonds between various pairs in the respective systems.

A40		
Energy	UA-AP	AP-MM
electrostatic	-538.76	-306.70
vdW	-162.15	-50.40

TABLE S5: The decompostion of total energy into its two components (i.e., electrostatic and vdW energies) for numerous pais. The energy is expreseed in kcal/mol unit.

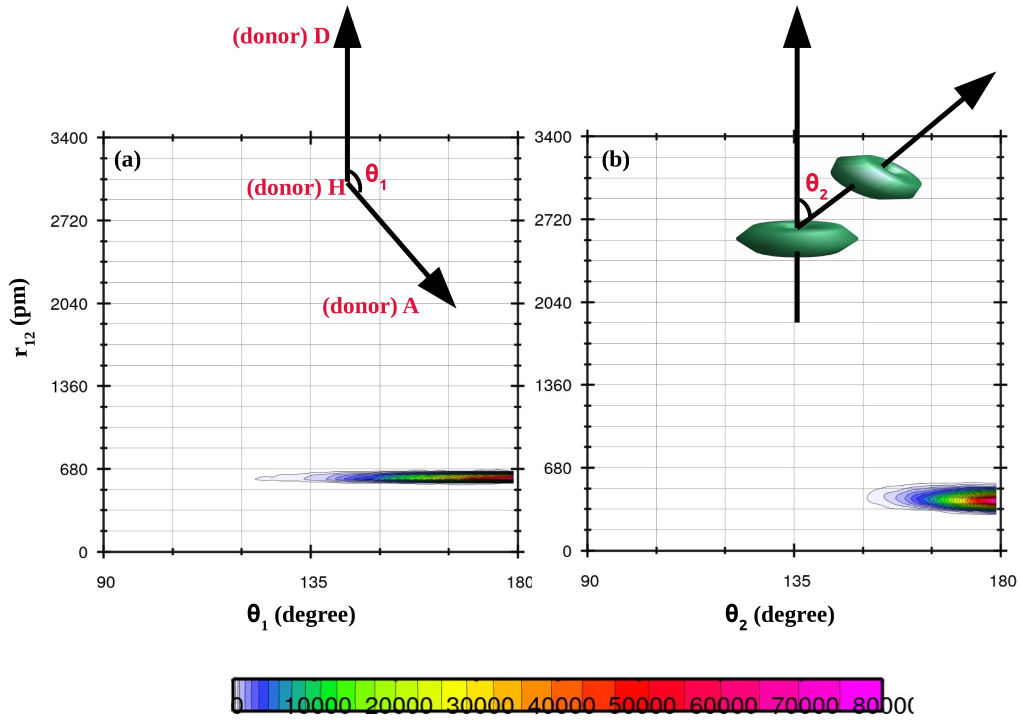

FIG. S19: In system A40, the distribution of orientational angle (θ_1) between UA and AP molecules considering two-point vectors (i.e. the vector connected by donor (D), hydrogen (H), and acceptor (A) atomes of these two molecules) to describe the hydrogen bonding phenomenon, (e) The angle between two vector normals (θ_2) between two aromatic ring is shown to present the π-stacking. Here, r_{12} refers to the center of mass (COM)- center of mass (COM) distance between the respective molecules.

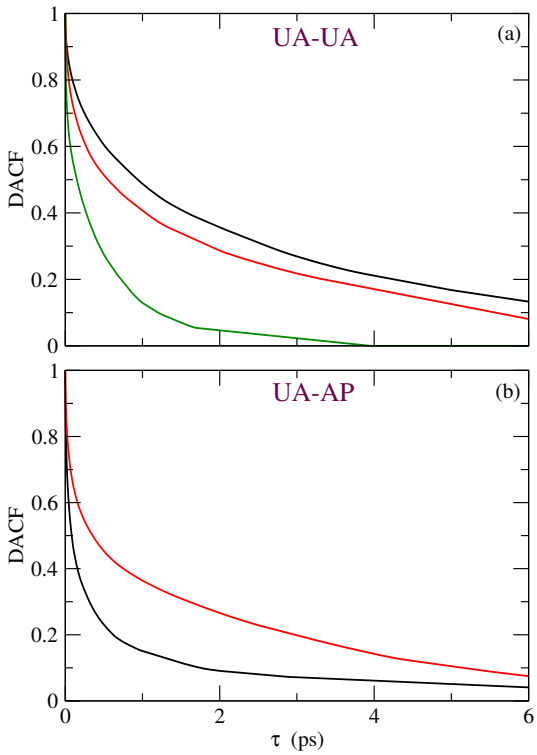

FIG. S20: DACF for (a) UA-UA (upper pannel) pair for systems T0 (black), A15 (red), and A40 (green) and (b) DACF for UA-AP (lower pannel) pair for systems A15 (black) and A40 (red).

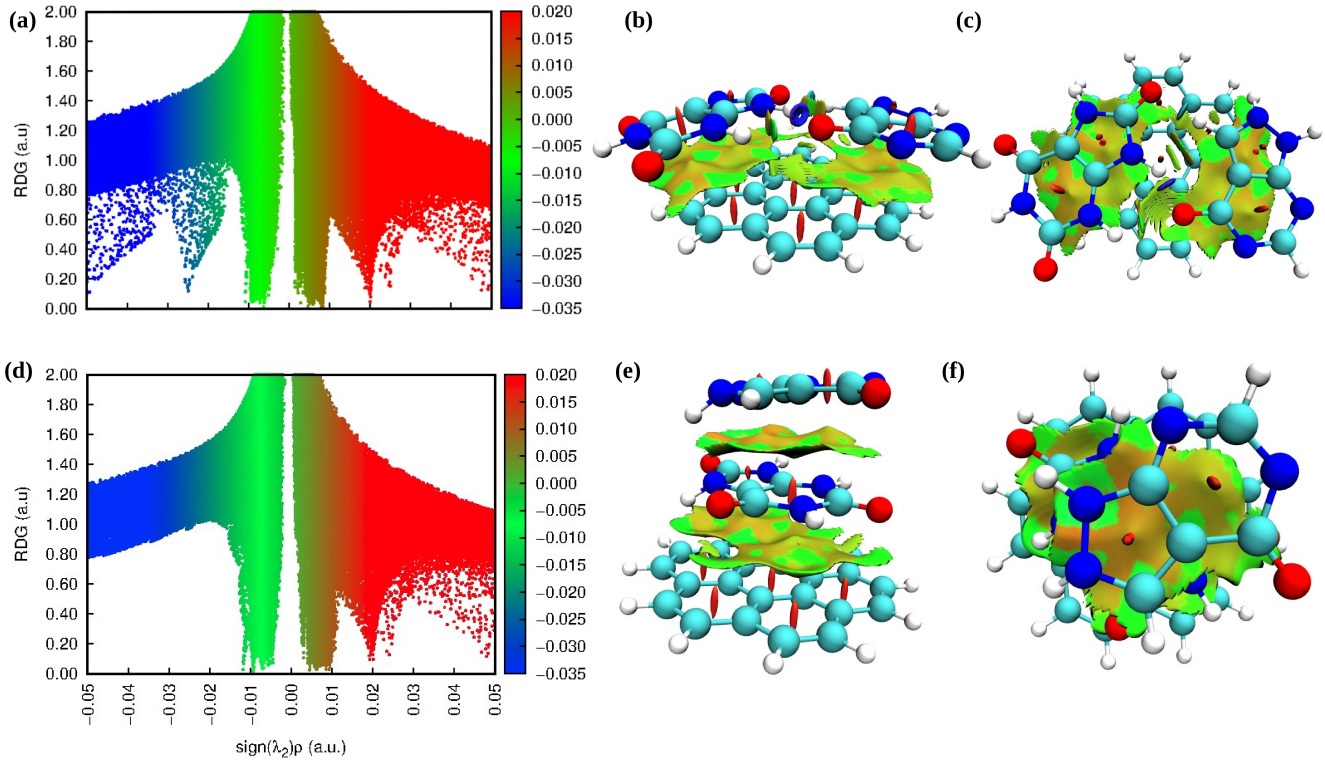

FIG. S21: Color-filled RDG isosurface reciprocates noncovalent interaction (NCI) regions for various interactions among UA, AP, and coronene system. (a)-(c) two hydrogen bonded UA and AP molecules are adsorbed over a coronene surface, and (d)-(f) two π-stacked UA and AP molecules are adsorbed over a coronene surface. The vertical axis of this plot is the reduced density gradient (RDG), and the horizontal axis is the sign of the second largest eigenvalue of the electron density Hessian matrix at position r (sign($\lambda_2(\rho)$). Here, the strong repulsive non-bonded steric interaction is observed in the red, and attractive interactions like the hydrogen bonding and van der Waals are blue and green.

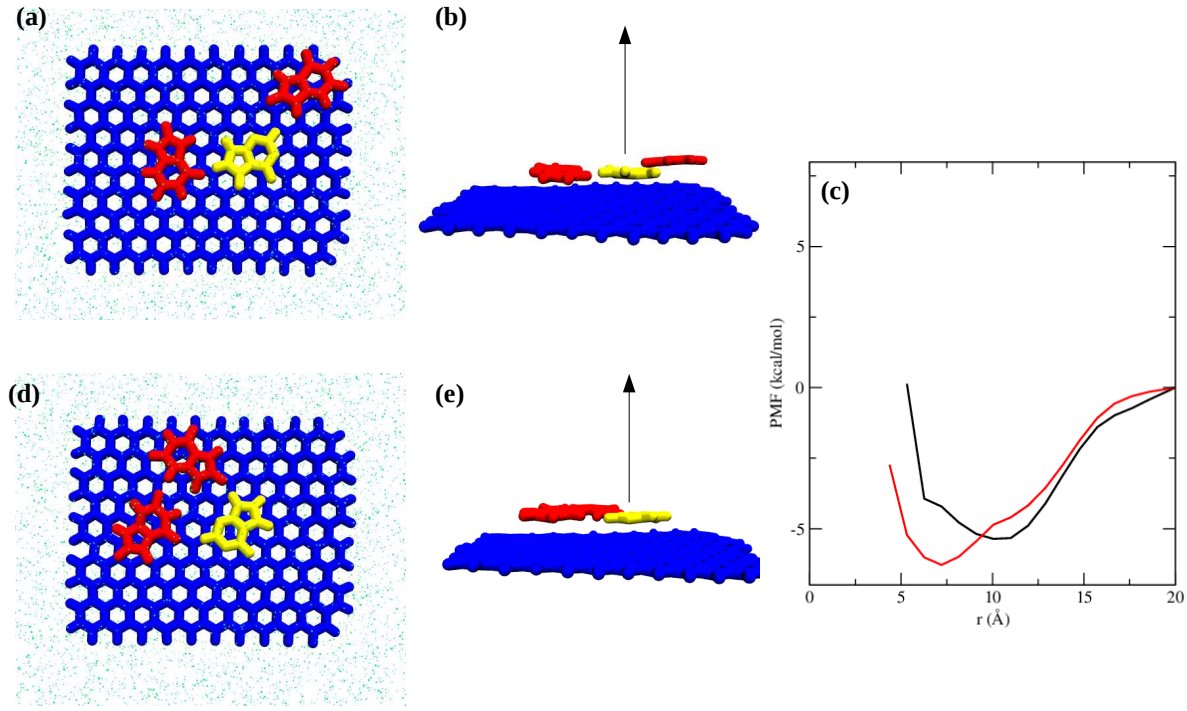

FIG. S22: (a) UA (red) and AP (yellow) molecules are adsorbed on a graphene surface in system U2A1G1, (b) AP molecule is pulled up from UA molecules in system U2A1G1, (c) PMFs for UA and AP interaction in systems U2A1G1 (black) and U2A1G1-a (red), (d) UA (red) and AP (yellow) molecules are adsorbed on a graphene surface in system U2A1G1-a, and (e) AP molecule is pulled up from UA molecules in system U2A1G1-a.

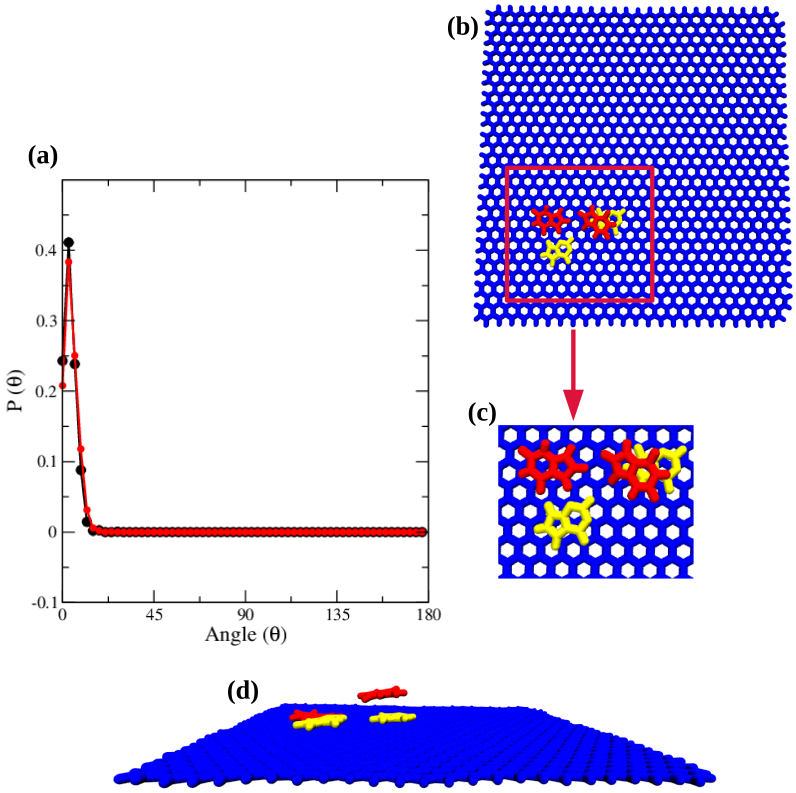

FIG. S23: (a) The probability of orientational angle (θ) between the vector normals of UA (black) and AP (red) molecules with the normal vector of graphene surface in system A15, (b)-(d) the adsorbed UA (red) and AP (yellow) molecules on the graphene sheet (blue) exhibit parallel orientation.

---

* Electronic address: sandipp@iitg.ernet.in